Available online at www.sciencedirect.com

ScienceDirect

Energy Procedia 69 (2015) 379 – 387

Energy Procedia

International Conference on Concentrating Solar Power and Chemical Energy Systems, SolarPACES 2014

Design optimization of a novel receiving cavity for Concentrated Solar Power applications by means of 3D CFD simulations

A. Gaetano[a], S.A. Zavattoni[a], M.C. Barbato[a,]*, P. Good[b], G. Ambrosetti[c], A. Pedretti[c]

[a]*Department of Innovative Technologies, SUPSI, Galleria 2, Manno 6928, Switzerland*
[b]*Department of Mechanical and Process Engineering, ETH Zurich, Sonneggstrasse 3, Zurich 8092, Switzerland*
[c]*Airlight Energy Manufacturing SA, Via Industria, Biasca 6710, Switzerland*

Abstract

The aim of this work was the design optimization, by means of accurate steady state 3D CFD simulations, of a novel receiving cavity for Concentrated Solar Power (CSP) applications. The receiving cavity has been developed by Airlight Energy Manufacturing SA in collaboration with ETH Zurich and SUPSI-DTI-ICIMSI within the framework of the SolAir-2 project. It is made of a helically coiled steel tube, and resulted highly effective in converting the radiative energy coming from the sun into thermal energy gathered by air which was selected as heat transfer fluid (HTF) being cheap, environmentally friendly and suitable for high temperatures applications.

The main geometrical parameters considered for the optimization were: cavity height, varied by increasing or decreasing the number of coils, cavity external diameter, and the presence of a spiral coiled tube closing the cavity top. For each configuration the air flow rate, with an inlet temperature of 120°C, was tuned in order to reach an outlet temperature close to the target value of 650°C. Cavity performance were evaluated in terms of thermal efficiency and pressure drop under two different skew angle conditions for the incoming solar radiation, 18° and 40°. CFD simulations were performed with Ansys Fluent. Navier-Stokes and energy equations were numerically solved using the finite-volume method approach; radiation heat transfer inside the cavity was taken into account by means of the Discrete Ordinates (DO) radiation model.

Peer review by the scientific conference committee of SolarPACES 2014 under responsibility of PSE AG

Keywords: receiving cavity, heat transfer, computational fluid dynamics simulation (CFD), air receiver.

* Corresponding author. Tel.: +41-058-666-6639.
E-mail address: maurizio.barbato@supsi.ch

Peer review by the scientific conference committee of SolarPACES 2014 under responsibility of PSE AG
doi:10.1016/j.egypro.2015.03.044

1. Introduction

The innovative parabolic trough collector (Fig. 1a) developed and built by Airlight Energy Manufacturing SA for its pilot plant, inaugurated on June 18th 2014 in Ait Baha (Morocco), is a completely new CSP solution [1, 2]. Besides the use of an inflated mirror with high optical efficiency, and of a sustaining structure made of precast fiber-reinforced concrete, the collector embeds a novel receiver (Fig. 1b) which includes a secondary optics coupled with two strings of helically coiled tubes exploited as receiving cavities. A thin ethylene tetrafluoroethylene (ETFE) sheet creates a controlled environment in which the inflated mirrors and the whole receiver are contained avoiding the problem of dust deposition on the primary mirrors.

As depicted in Fig. 1c, showing a schematic of the system working principle, the solar radiation collected by the primary mirror is further concentrated by a high efficiency secondary optics into the receiving cavity aperture; a glass window separates the cavity interior from the external environment reducing the thermal loss due to convection and back-radiation. The cavity walls heated up by the sunrays, transfer the thermal energy to the flowing air, which is fed into the coiled tube from the bottom at a temperature of 120°C, and reaches up to 650°C. A run-back pipe, thermally insulated by means of radiative shields [3], collects the hot air coming from the different receiving cavities placed all along the receiver length. The air flow is then used to feed a steam generator.

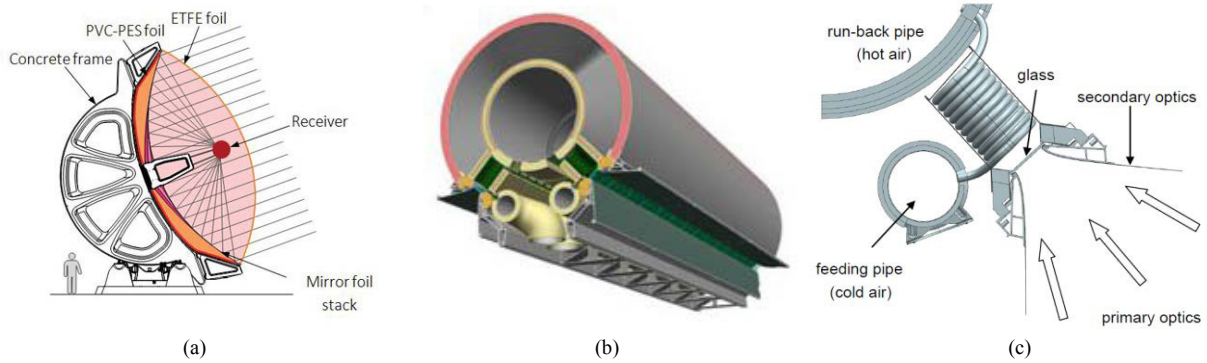

Fig. 1: Airlight Energy Manufacturing SA solar collector (a), receiver (b), receiving cavity (c).

2. Receiving cavity

The receiving cavity, very effective in transforming the solar energy into thermal energy gathered by the HTF, is basically made of three main components: a helically coiled tube, a glass window and the secondary optics.

The tube, with an internal diameter of 11 mm and a thickness of 0.5 mm, is made of stainless steel to withstand the high temperatures. Its helical shape, adopted to form the receiving cavity, also allows to exploit the two main advantages of a gas flowing through a coiled pipe: a) an enhanced heat transfer coefficient with respect to straight tubes (for the same flow condition) and b) a stabilizing effect on the flow regime moving forward the critical Reynolds number for laminar to turbulent transition [4] with beneficial effects on the required pumping power. To maximize the absorption of the solar radiation the external surface of the steel pipe was black painted. A solid insulation material surrounds the coiled tube to avoid thermal loss towards the external environment.

The glass window, with a thickness of 3.3 mm, was treated with an anti-reflective coating to minimize losses of the radiation focused by the hyperbolic secondary optics whose surfaces are coated with a silver film for a better reflective behavior. A water cooling circuit keeps the temperature of the silver coating below the limit of 120°C preserving the optimal optics characteristics.

The geometrical parameters considered for the cavity optimization were the cavity height, the cavity external diameter and the presence of a spiral coiled tube closing the cavity top; all of them are schematically represented in Fig. 2. Table 1 summarizes the different configurations analyzed by means of CFD simulations.

Fig. 2 Receiving cavity optimization parameters: with top spiral (l.h.s.) without top spiral (r.h.s.)

Table 1: Optimization parameters

Optimization parameters				
Parameter	**Case 1**	**Case 2**	**Case 3**	**Case 4**
Cavity height [mm]	96	144	144	144
Cavity external diameter [mm]	112	112	92	92
Top spiral	yes	yes	yes	no

The cavity performance were evaluated in terms of pressure drop and system thermal efficiency defined as the ratio between the power gathered by the air flow and that absorbed by the cavity internal walls.

3. CFD modeling

3.1. Computational domain definition

The computational domain considered for the optimization study was limited to the helically coiled pipe and the glass window in order to reduce the computational time and better focusing on the main thermodynamic effects, i.e. the air heating and the thermal loss through the glass window.

To avoid the presence of highly distorted cells in the computational grid (see Fig. 3 l.h.s.), it was not possible to directly model the pipe with its real helical shape. Therefore its geometry was simplified replacing the coils by means of a series of annular hollow cylinders placed one above the other (Fig. 3 r.h.s). In order to allow the air flow through the different elements each of them was coupled with the one right above by means of a periodic boundary condition; the flow parameters at one end of the a certain annular hollow cylinder were then assumed as inputs for the one placed above it. The solid zones, representing the coiled steel tube, were coupled as well.

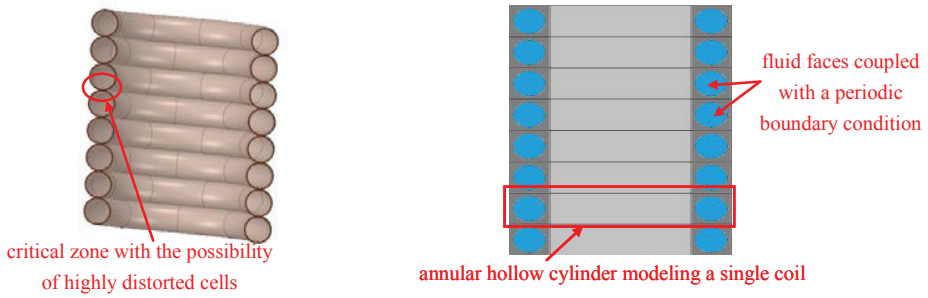

Fig. 3: Pipe real shape (l.h.s.), pipe CFD model (r.h.s.).

The spiral pipe closing the cavity top was also simplified. In this case the pipe was modeled by means of concentric disks. Fig. 4 depicts the final computational domain implemented for Case 1 (see Table 1) highlighting

the different zones. The glass window, made of Borofloat® [5], is supported by a steel structure which was also modeled. A high quality mesh was generated, with local refinement applied in the most critical regions (helically coiled pipe, air volume boundaries and glass window).

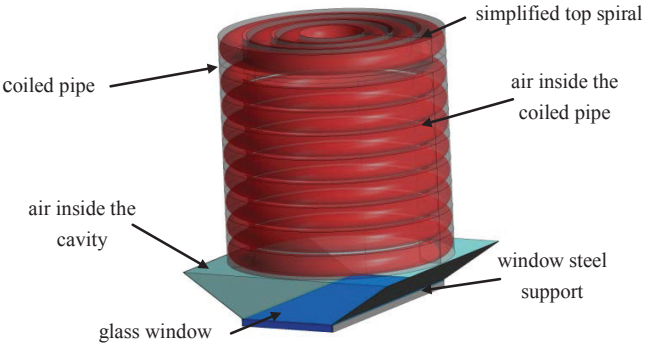

Fig. 4: Computational domain for Case 1.

3.2. Boundary conditions

The solar radiation collected by the primary mirror and further concentrated by the secondary optics was modeled as a volumetric power source onto the cavity internal walls and distributed according to the results of a ray-tracing analysis. Two cases for the skew angle of the solar radiation were considered: 18° and 40°. For the first one, the input power was assumed to be uniformly distributed upon one half of the cavity internal surfaces and on the cavity top (see Fig. 5) while for the latter the power distribution varies linearly going from zero at the cavity top to its maximum value close to the glass window; only a quarter of the cavity internal surfaces is hit by the solar radiation in this case and, depending on the cavity height, some of the top coils are not illuminated.

A mass flow rate at 120°C was assumed as boundary condition for the inlet section and its value was tuned for each different case in order to achieve an air outlet temperature close to the target value of 650°C.

The external walls of the coiled pipe were set to be adiabatic. The heat loss through the glass window due to convection and radiation was modeled by assuming on the glass external surface a boundary condition in which the reference temperatures used to compute the radiative and convective heat losses were both set to 70°C, which is the temperature of the controlled environment created by the ETFE foil. Since wind does not directly affect the receiving cavities, a convective heat transfer coefficient of 4 W/m^2K was assumed. According to the data provided by the supplier, the emissivity of the glass window was set to 0.83.

As depicted in Fig. 5 a periodic boundary condition was also applied on the lateral faces of the volume modeling the air zone between the cavity and the glass window in order to take into account the heat exchange due to the presence of adjacent cavities.

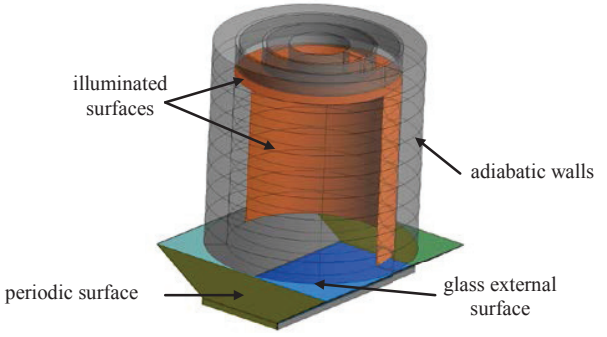

Fig. 5: Boundary conditions for Case 1 (see Table 1) for 18° skew angle condition

3.3. Materials characteristics, modeling equations and numerical schemes

Air was modeled as an ideal gas and its thermo-physical properties were assigned as piecewise linear interpolation of data available in literature [6]. Glass thermal conductivity was implemented as indicated by the supplier [4]. For all the mass flow rate conditions studied the flow Mach number is always lower than 0.3. Therefore the air flow was simulated as incompressible [7] and the particular cavity shape also keeps it in laminar regime.

Navier-Stokes and energy equations were numerically solved by means of the finite-volume method approach used in Ansys Fluent. Radiation heat transfer between the cavity internal walls and between the cavity walls and the glass window was modeled by means of the Discrete Ordinates (DO) radiation model [8, 9] assuming an angular discretization of 2 for both theta and phi divisions which can be considered acceptable for most practical problems [10]; theta and phi pixels were set to 3.

4. CFD simulations results

4.1. 18° skew angle condition

Table 2 reports the main input parameters set to run the CFD simulations together with the most important results obtained for the 18° skew angle condition.

Table 2: Simulations results for the 18° skew angle condition

Cavity optimization – 18° skew angle				
Input parameters	**Case 1**	**Case 2**	**Case 3**	**Case 4**
Cavity height [mm]	96	144 mm	144	144
Cavity external diameter [mm]	112	112	92	92
Top spiral	yes	yes	yes	no
Mass flow rate [kg/s]	6.216E-04	6.216E-04	5.33E-04	5.33E-04
Air inlet temperature [°C]	120	120	120	120
Input power [W]	406.13	406.13	333.59	333.59
Simulation results	**Case 1**	**Case 2**	**Case 3**	**Case 4**
Pressure drop [Pa]	1’589	2’250	1’431	1’221
Air outlet temperature [°C]	656.35	661.85	650.55	650.38
Power absorbed by the air flow [W]	356.35	360.13	302.24	302.18
Power lost through the glass window [W]	49.78	46	31.35	31.41
Thermal efficiency [-]	0.877	0.886	0.906	0.905

The first analysis was carried out to assess the effect of a variation of the cavity height on the receiving cavity performance. As reported in Table 2, two values were considered: 96 mm (Case 1) and 144 mm (Case 2). As expected the resulting pressure drop is higher for Case 2 because of the greater length of the helically coiled pipe; four more coils, with respect to Case 1, were indeed added to increase the cavity height (for the same cavity external diameter). A slight increment of the system thermal efficiency was also observed mainly due to a difference in the input power distribution. In Case 2 most of the incoming solar radiation, directly illuminates the coils with a small fraction hitting the top spiral leading to a more effective air heating. The top spiral is also farther from the glass window allowing a reduction of the heat loss through it.

In order to further reduce the thermal loss through the glass window, the cavity external diameter was reduced going from 112 mm of Case 2 to 92 mm of Case 3. The input power is also different between the two cases because a smaller fraction of the solar radiation is actually entering the receiving cavity; therefore the mass flow rate was tuned accordingly. The cavity height was kept to 144 mm. Case 3 shows a further increment of about 2% in terms of thermal efficiency while the pressure drop obviously decreases due to the shorter length of the helically coiled pipe.

With the aim of reducing the system pressure drop without affecting the gain in thermal efficiency obtained so far, a model without the top spiral was designed and simulated. As depicted in Fig. 6 the cavity top in Case 4 of Table 2 was assumed to be closed by means of a flat steel cap.

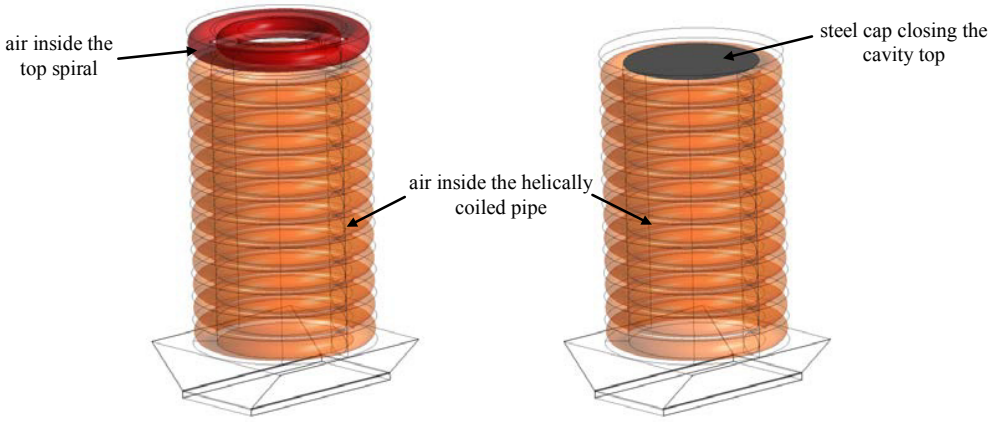

Fig. 6: Geometry comparison between Case 3 (l.h.s) and Case 4 (r.h.s)

As reported in Table 2 the removal of the top spiral didn't affect much the system thermal efficiency meaning that most of the air heating takes place while it flows through the coils with a minor contribution, in terms of temperature increment, given by the top spiral.

Figure 7 shows the improvement in thermal efficiency obtained passing from the configuration of Case 1 to that of Case 4 which was finally chosen as optimized geometry.

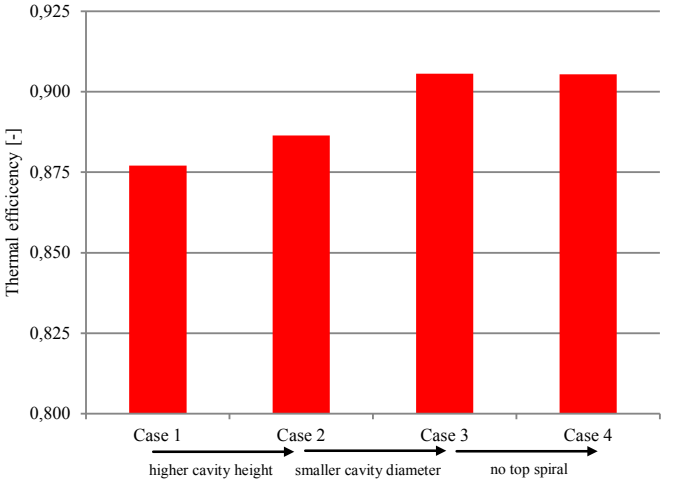

Fig. 7: Thermal efficiency increment

4.2. 40° skew angle condition

Additional CFD simulations were run to verify the effectiveness of the optimized geometry for the 40° skew angle condition. Table 3 compares the results of this study for Case 1 and Case 4. The optimized design maintains a higher thermal efficiency with respect to the initial one albeit the overall gain is now limited to 1.6%.

A reduction of about 20% can however be seen when comparing the final geometry performance at 18° (see Table 2) and 40° skew angle conditions. This difference can be understood by thinking at the input power

distribution. With the higher skew angle, the solar radiation illuminates only a quarter of the cavity internal walls and it is mainly focused on the lower coils. This condition has the effect of creating a high temperature region close to the glass window, illustrated in Fig. 8, with a consequent increment of the heat losses causing a significant reduction of the system thermal efficiency.

Table 3: Simulations results for the 40° skew angle condition

40° Skew Angle		
Input parameters	**Case 1**	**Case 4**
Cavity height [mm]	96	144
Cavity external diameter [mm]	112	92
Top spiral	yes	no
Mass flow rate [kg/s]	4.02E-04	3.41E-04
Air inlet temperature [°C]	120	120
Input power [W]	309.9	253.9
Simulation results	**Case 1**	**Case 4**
Pressure drop [Pa]	964	746
Air outlet temperature [°C]	648.9	640.59
Power absorbed by the air flow [W]	227.56	190.44
Power lost through the glass window [W]	82.34	63.46
Thermal efficiency [-]	0.734	0.750

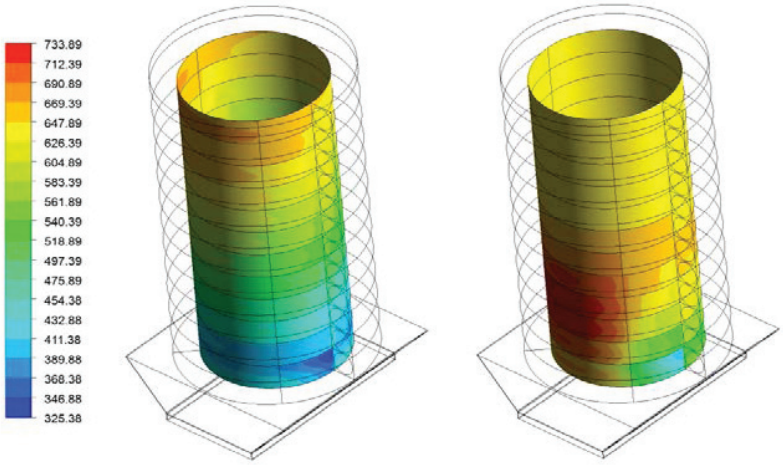

Fig. 8: Optimized geometry, temperature contours (in °C) comparison: 18° skew angle (l.h.s) 40° skew angle (r.h.s).

5. Real design

Based on the results of the optimization study a more detailed model of the receiving cavity was created (see Fig. 9). The secondary optics with its water cooling circuit and the insulation material surrounding the helically coiled tube were also considered. The air volume between the glass window and the secondary optics itself was also implemented to take into account the radiation heat transfer between the two surfaces.

The system was simulated under realistic working conditions for a 18° skew angle condition. Again the mass flow rate was tuned to meet the requirement of a 650°C outlet temperature.

The flow regime remains laminar. The modeling equations and the numerical schemes were the same adopted during the optimization phase [11].

The main simulation results, reported in Table 4, show a 10% reduction of the system thermal efficiency with respect to the simplified model of Case 4 (see Table 2). The reason of that is twofold: the first one is the presence of the water cooling circuit for the secondary optics which not only absorbs the power not reflected by the external surface but also that coming from the high temperature internal parts of the receiving cavity; the second one is that the external surfaces of the receiving cavity are now in contact with the external environment causing an additional heat loss due to convection and radiation. The thermal efficiency however, still remains quite high highlighting the effectiveness of this design concept in harvesting the solar energy.

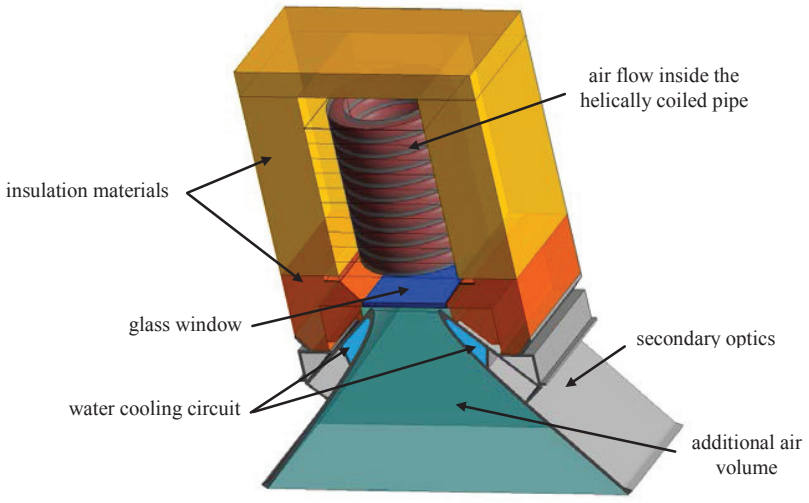

Fig. 9: Real model - computational domain main elements

Table 4: Real model simulation results [10].

Real model at 18°skew angle condition	
Input	
Cavity height [mm]	120
Cavity external diameter [mm]	92
Top spiral	No
Mass flow rate [kg/s]	4.7E-04
Air inlet temperature [°C]	120
Input power [W]	333.6
Simulation results	
Pressure drop [Pa]	876
Air outlet temperature [°C]	655.3
Power absorbed by the air flow [W]	269.2
Power absorbed by the cooling circuit[W]	31.3
Power lost towards the external environment [W]	33.1
Thermal efficiency [-]	0.806

6. Conclusions

The design of a receiving cavity for CSP applications made of a helically coiled pipe was optimized by means of 3D steady state CFD simulations and tested under two different conditions for the skew angle of the solar radiation. A simplified model, taking into account the helically coiled pipe and the glass window only, was created in order to reduce the computational time while all the relevant phenomena were modeled. Among the three geometrical parameters considered (cavity height, cavity external diameter and presence of the top spiral) the one leading to the

great improvement (2%) in terms of thermal efficiency was the reduction of the cavity external diameter, which had the greatest effect in reducing the thermal losses through the glass window. The top spiral was also removed in order to decrease the system pressure drop. For a 40° skew angle the gain in efficiency was limited to 1.6% but still with a quite high overall value above 70%.

The optimized design was then adopted to create a more detailed model including also the secondary optics, their cooling circuit and the insulating materials surrounding the cavity. A decrement of the thermal efficiency with respect to the simplified model was seen in this case due to the additional losses introduced by the presence of the water cooling circuit and to the thermal losses towards the external environment. The thermal efficiency however remains quite high and, in the most favourable condition of 18° skew angle is about 0.8.

Acknowledgements

This work has been developed in the framework of the SolAir-2 project (project “SI/500091”) financed by the Swiss Federal Office of Energy (SFOE - OFEN - BFE) under the contract numbers “SI/500091-01”.

Reference

[1] Pedretti A., ”A 3 MW thermal concentrated solar power pilot plant in Morocco with the Airlight Energy technology” SolarPACES 2012, Marrakech, Morocco.
[2] Good P., Zanganeh G., Ambrosetti G., Barbato M. C., Pedretti A., Steinfeld A., “Towards a commercial parabolic trough CSP system using air as heat transfer fluid”, Energy Procedia, vol. 49, pp. 381 – 385, 2014
[3] Montorfano D., Barbato M. C., Gaetano A., Pedretti A., Malnati F. Pusterla S., “Thermal insulation based on radiation shields for CSP-HTF pipes: CFD modeling and experimental validation”, SolarPACES 2012, Marrakech Morocco.
[4] Dean W.R., “The stream-line motion of fluid in a curved pipe”, Philosophical Magazine 7, Vol. 5, Issue 30, pp. 673-695, 1928.
[5] “www.schott.com/borofloat/english/?highlighted_text=borofloat,” [Online].
[6] Incropera, F. P., D.P. Dewitt, T.L. Bergman, and A.S. Lavine. “Fundamentals of heat and mass transfer, 6th edition”, John Wiley & Sons, 2007.
[7] Anderson J.D., “Fundamentals of aerodynamics - Fourth edition”, McGraw-Hill, 2007.
[8] Raithby G.D., Chui E.H., “A finite-volume method for predicting a radiant heat transfer in enclosures with participating media” Journal of Heat Transfer, Vol. 112, pp. 415–423, 1990.
[9] Chui E.H., Raithby G.D., “Computation of radiant heat transfer on a non-orthogonal mesh using the finite-volume method”, Numerical Heat Transfer, Part B, Vol. 23, pp. 269–288, 1993.
[10] Fluent 14.5 User’s Guide.
[11] Zavattoni S.A., Gaetano A., Barbato M.C., Ambrosetti G., Good P., Malnati F., Pedretti A., “CFD analysis of a receiving cavity suitable for a a novel CSP parabolic trough receiver”, Energy Procedia, vol. 49, pp. 579-588,2014.